Clin Neuroradiol (2016) 26:347–353
DOI 10.1007/s00062-014-0361-z

ORIGINAL ARTICLE

Ecchordosis Physaliphora: Evaluation with Precontrast and Contrast-Enhanced Fast Imaging Employing Steady-State Acquisition MR Imaging Based on Proposed New Classification

A. Özgür · K. Esen · E. Kara · E. Yencilek · Y. Vayisoğlu · T. Kara · A. Yıldız

Received: 15 September 2014 / Accepted: 18 November 2014 / Published online: 10 December 2014

Abstract
Purpose Ecchordosis physaliphora (EP) is a notochordal remnant typically located at the dorsal surface of the clivus, which has to be distinguished from the other retroclival lesions. Our aim is to investigate the imaging features of intracranial EP using precontrast and contrast-enhanced fast imaging employing steady-state acquisition (FIESTA).
Methods We retrospectively evaluated the precontrast and contrast-enhanced FIESTA images of 399 patients with temporal magnetic resonance imaging to detect "classical EP" and "possible EP." The classical EP was classified into type A (hyperintense excrescence (cyst-like component) on the dorsal surface of the clivus) and type B (hyperintense excrescence plus a hyperintense lesion within the clivus). Possible EP was subdivided as incomplete EP (T2-hypointense protrusion of the clivus) and EP variant (hyperintense lesion within the clivus alone).
Results We found 31 (31 of 399, 7.7%) EPs of which 11 were defined as classical EP (2.7%) and 20 were defined as possible EP (5.0%). Of the 11 classical EPs, 7 (63.6%) were diagnosed as type A and 4 (% 36.4) were diagnosed as type B. Of the 20 possible EPs, 19 were classified as incomplete EP (95.0%) and one was classified as EP variant (5.0%).
Conclusions Contrast-enhanced FIESTA images are helpful in the assessment of EP, although we do not define a role in the current classification proposed by Chihara et al. (Eur Radiol 23:2854–2860, 2013).

Keywords Ecchordosis physaliphora · FIESTA · MRI · Temporal MR

A. Özgür (✉) · K. Esen · E. Kara · T. Kara · A. Yıldız
Department of Radiology, Mersin University Faculty of Medicine,
34. Cadde, Çiftlikköy Kampüsü,
33343 Mersin, Turkey
e-mail: anilozgur@yahoo.com

E. Yencilek
Department of Radiology, Haydarpaşa Numune Training and Research Hospital,
İstanbul, Turkey

Y. Vayisoğlu
Department of Otorhinolaryngology, Mersin University Faculty of Medicine,
Mersin, Turkey

Introduction

Ecchordosis physaliphora (EP) is a rare, congenital, benign lesion derived from notochordal tissue that is typically located at the midline of the craniospinal axis [1, 2]. This ectopic notochordal remnant is most commonly found in the intradural space of the prepontine cistern with an attachment to the dorsal surface of the clivus [1, 2]. Intracranial EP is usually an incidental finding on imaging studies that has to be differentiated from other retroclival lesions including chordoma.

In radiology literature, there are few studies that investigate the prevalence and the imaging features of intracranial EP in large series of patients [3, 4]. In 2004, Mehnert et al. [3] reported five patients with retroclival EP on magnetic resonance (MR) imaging using thin-section T1-weighted and T2-weighted images. In all cases, EP showed high signal on T2-weighted images, low signal on T1-weighted images, and no contrast enhancement. Although MR sequences used in this study may yield excellent soft-tissue resolution, their spatial resolution is inadequate to evaluate small intracranial lesions. Therefore, it is unlikely to understand imaging

features of intracranial EP completely based on these traditional MR sequences.

Balanced steady-state free precession (SSFP) techniques such as fast imaging employing steady-state acquisition (FIESTA), constructive interference in a steady state (CISS), and true fast imaging with steady-state free precession are now commonly used in MR imaging. These sequences provide strong signal in tissues with high T2/T1 ratio such as cerebrospinal fluid (CSF) and high spatial resolution with submilimetric section thicknesses allowing the reconstruction of multiplanar images [5, 6]. Therefore, SSFP sequences are capable of depicting tiny intracranial lesions in contrast to the traditional MR techniques.

In a recent study, Chihara et al. [4] retrospectively investigated the imaging findings of EP using FIESTA sequence. With the full advantage of this imaging technique, they described diverse imaging features and proposed a new classification for EP. Lesions were defined as classical EP type A (hyperintense excrescence (cyst-like component) on the dorsal surface of the clivus), classical EP type B (hyperintense excrescence plus a hyperintense lesion within the clivus), incomplete EP (EP bud: T2-hypointense protrusion of the clivus), and EP variant (hyperintense lesion within the clivus alone). However, contrast-enhanced images were not available in most of their patients. FIESTA sequence, in addition to its strong T2 contrast, may also provide T1 contrast and show increased signal intensity correlated with the increase in gadolinium-based contrast agent concentration [7, 8]. Although FIESTA images without contrast administration may be adequate to detect small lesions, contrast-enhanced images are also necessary to rule out solid lesions such as chordoma, which otherwise mimic EP with its similar MR signal characteristics. Moreover, contrast-enhanced FIESTA sequence is also useful in distinguishing tumors arising from the dura or skull base from surrounding structures such as dura, bony degeneration, or venous sinuses [8–10]. Enhancement of the venous sinuses adjacent to the clivus on contrast-enhanced FIESTA may enable a better delineation of the bone cortex, resulting in clear visualization of T2-hypointense protrusion (incomplete EP) and reliable discrimination of intraclival lesions (EP variant) from surrounding structures. Therefore, we aimed to investigate the imaging features of intracranial EP using both precontrast and contrast-enhanced FIESTA images, which are routine sequences of our temporal MR imaging protocol.

Materials and Methods

Patients and Clinical Data

This study was approved by the ethics committee of our institution. Our retrospective review of the radiology database revealed 399 patients who underwent temporal MR imaging between January 2013 and March 2014. All patients were referred to our department due to vertigo, tinnitus, hearing loss, or follow-up of a known vestibular schwannoma. After re-reading of all studies, patients with low-quality MR images due to the motion or flow artifacts and a history of skull base disease or surgery were excluded. Two patients with prepontine epidermoid and a patient with a small midline retroclival and intraclival enhancing lesion were also excluded. Patients with nonenhancing hyperintense excrescence (cyst-like component) on the dorsal wall of the clivus, T2-hypointense protrusion of the clivus, and nonenhancing hyperintense lesion within the clivus were included in the study. A total of 31 patients (16 male, 15 female) with the ages ranging from 17 to 78 years (mean, 45.6 years) were found.

MR Imaging Protocol

All temporal MR examinations were performed at 1.5-T MR device (Signa Excite, GE Medical Systems, Milwaukee, WI, USA) with a dedicated eight-channel phased-array coil (USA Instruments, Aurora, OH, USA). Axial T1-weighted, T2-weighted, FIESTA, post-contrast FIESTA, post-contrast axial, and coronal T1-weighted images are obtained for standard temporal MR examination in our department. Our imaging parameters were as follows: T1 weighted (repetition time (TR), 650 ms; echo time (TE), 15.7 ms; slice thickness, 3 mm; interslice gap, 0.5 mm; field of view (FOV), 20 × 20 cm; matrix, 288 × 192; number of excitations (NEX), 2; bandwidth, ±31.2 kHz), T2 weighted (TR, 4725 ms; TE, 102 ms; slice thickness, 3 mm; interslice gap, 0.5 mm; FOV, 20 × 20 cm; matrix, 288 × 224; NEX, 2; bandwidth, ±22.7 kHz), FIESTA (TR, 5.1 ms; TE, 1.4 ms; slice thickness, 0.8 mm; FOV, 20 × 20 cm; matrix, 320 × 224; NEX, 2; bandwidth, ±62.5 kHz; flip angle, 55°)

Contrast-enhanced FIESTA and T1-weighted images were available in all selected patients. For contrast-enhanced images, gadodiamide hydrate (Omniscan; Daiichi Pharmaceutical Co., Tokyo, Japan), gadopentate dimeglumine (Magnevist; Bayer Schering-Pharma, Berlin, Germany), or gadoterate meglumine (Dotarem; Guerbet, Roissy, France) was administered as the intravenous contrast agent at 0.1 mmol/kg of body weight.

All precontrast and contrast-enhanced FIESTA images were obtained in axial plane. Coronal and sagittal reconstructed images of all patients were also created for assessment of the FIESTA images.

Analysis of MR Images

All MR images were carefully evaluated on high-resolution monitors by two radiologists (Anıl Özgür and Engin

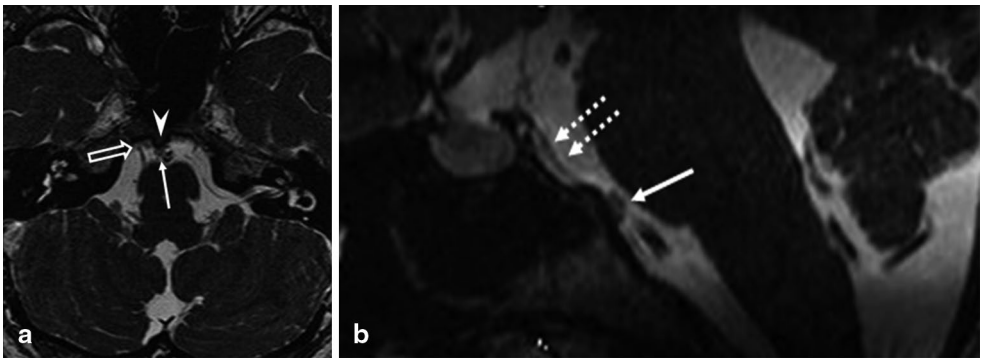

Fig. 1 Type A classical ecchordosis physaliphora in a 47-year-old man with vertigo. Axial (**a**) and reformatted sagittal (**b**) contrast-enhanced fast imaging employing steady-state acquisition images show a tiny, oval, cyst-like lesion (*arrow*) adjacent to the T2-hypointense protrusion (*arrowhead*) at the level of Dorello canal (*open arrow*) in the midline retroclival location. Note the enhancement within the basilar venous plexus (*dashed arrows*)

Kara, with 5 and 9 years of experience in neuroradiology, respectively) who were blinded to patient information. Initial evaluations were made independently, and inconsistencies were resolved by consensus with collaborative review. Lesions were categorized as "classical EP" and "possible EP" using the classification proposed by Chihara et al. [4]. The classical EP was further classified into type A (hyperintense excrescence (cyst-like component) on the dorsal surface of the clivus) and type B (hyperintense excrescence plus a hyperintense lesion within the clivus). Possible EP was also subdivided as incomplete EP (EP bud = T2-hypointense protrusion of the clivus) and EP variant (hyperintense lesion within the clivus alone). Subsequently, imaging features including location, size, and shape of all lesions associated with clinical presentations were noted for detailed evaluation.

Results

Two radiologists detected a total of 31 lesions by consensus after reviewing temporal MR images of 399 patients (31 of 399, 7.7%). Inconsistencies were only seen in the determination of the incomplete EP lesions in rare cases. Of the 31 patients with EP, MR examinations were performed for tinnitus ($n=14$), vertigo ($n=10$), hearing loss ($n=4$), and follow-up of a vestibular schwannoma ($n=3$). From among 31 lesions, 11 were defined as classical EP (11 of 399, 2.7%), and the remaining 20 were defined as possible EP (20 of 399, 5.0%); 26 (26 of 31, 83.9%) lesions were found at exactly the same level as the Dorello canal, and the remaining 5 (5 of 31, 16.1%) were detected at an upper level. All EPs were located at the midline of the craniospinal axis.

Classical EP

Patients with classical EP ($n=11$) were referred to our department for tinnitus ($n=7$), vertigo ($n=2$), hearing loss ($n=1$), and vestibular schwannoma ($n=1$). The transverse size of the lesions ranged from 1.5 to 8.4 mm. Of the 11 classical EPs, 7 (63.6%) were classified as type A and 4 (36.4%) were classified as type B.

The hyperintense excrescences were oval-shaped ($n=9$, 81.8%; Fig. 1) or lobulated ($n=2$, 18.2%). All lesions were located at the midline; however, three of the lesions demonstrated superior, inferior, and right paramedian superior extensions, respectively, when considering the attachments of the lesions to the dorsal surface of the clivus. Furthermore, in three of the oval-shaped lesions, the walls of the EPs were displaced by the adjacent basillary artery in two patients with tinnitus and vertigo, respectively, and by the anterior inferior cerebellary artery in one patient with tinnitus. Of the two lobulated lesions, one was clearly visible on axial image, while another was best seen on reformatted sagittal image.

In two of the type B EPs, hyperintense lesions within the clivus were divided into two parts by a midline bony segment (Fig. 2). This bifid appearance of the intraclival lesion was seen on axial and sagittal planes in two patients, respectively.

All type A lesions and two (2 of 4, 50%) of the type B lesions were in association with T2-hypointense protrusion of the clivus. All classical EPs were seen at the Dorello canal level except one of the type A lesions. In only one patient, previous MR examination performed at 1 year ago was available. The lesion showed no interval change.

Possible EP

In a total of 20 lesions consistent with possible EP, all but one were classified as incomplete EP ("EP bud"; 19 of 20, 95.0%; Fig. 3). Among the incomplete EPs, 16 (16 of 19, 84.2%) were located at the same level as the Dorello canal and three (3 of 19, 15.8%) were found to be at an upper level.

Only one (1 of 20, 5.0%) patient was evaluated as EP variant (Fig. 4). The intraclival lesion of this patient was located in the midline at an upper level than the Dorello canal. The patient was presented with unilateral hearing loss.

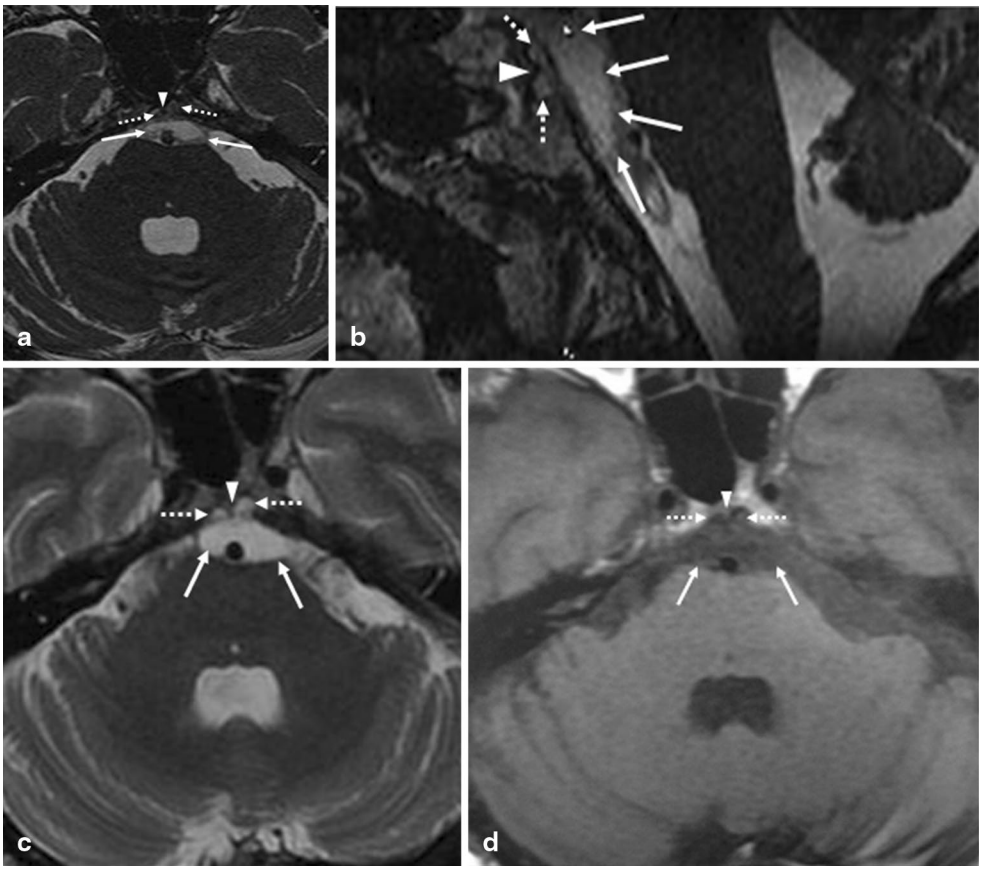

Fig. 2 Type B classical ecchordosis physaliphora in a 54-year-old man with tinnitus. Axial (**a**) and reformatted sagittal (**b**) contrast-enhanced fast imaging employing steady-state acquisition images demonstrate a large cystic lesion (*arrows*) occupying the prepontine cistern in communication with an intraclival hyperintense lesion (*dashed arrows*). Note the bifid appearance of the hyperintense lesion within the clivus caused by a midline bony segment (*arrowhead*). Axial T2-weighted (**c**) and T1-weighted (**d**) images also reveal the retroclival lesion (*arrows*) associated with the intraclival lesion (*dashed arrows*) divided by a midline bony segment (*arrowheads*)

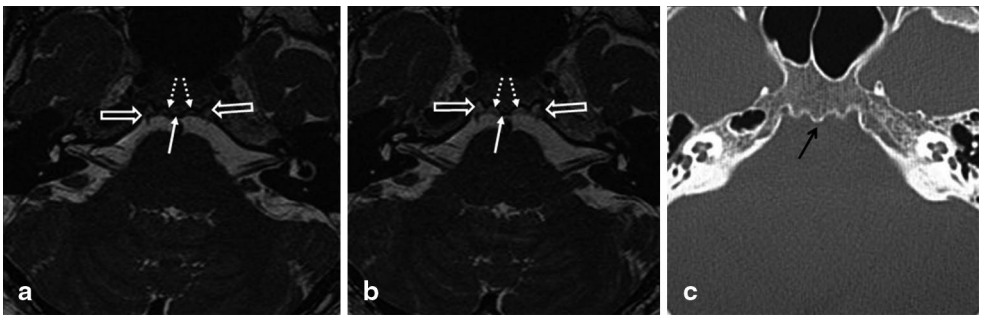

Fig. 3 Incomplete ecchordosis physaliphora (EP; EP bud) in a 53-year-old woman with vertigo. Axial precontrast (**a**) and contrast-enhanced (**b**) fast imaging employing steady-state acquisition images show T2-hypointense protrusion of the clivus (*arrow*) in the midline associated with the basilar venous plexus (*dashed arrows*) at the Dorello canal level (*open arrows*). Note the better visualization of the T2-hypointense protrusion of the clivus between the enhancing basilar venous plexus on contrast-enhanced image. Computed tomography (**c**) reveals the clival bony spur (*black arrow*)

Discussion

In the present study, we found 31 lesions with diverse imaging findings including 11 classical EPs and 20 possible EPs after reviewing 399 temporal MR examinations. The overall incidence of EP (7.7%) in this study is similar to the incidence (8.0%) found by Chihara et al. [4]. However, the incidence of classical EP in our study (2.7%) is slightly higher than those detected by the previous two imaging studies [3, 4], which respectively revealed identical incidence (1.7%). Although we do not know the exact cause of higher incidence of classical EP in our study, the reason may be related to the study population, which included symptomatic patients who were referred for temporal MR imaging. Although EP is usually asymptomatic, some cases with different symptoms including headache, dizziness, CSF fistula, subarachnoidal hemorrhage, diplopia, or abducens nerve palsy have been reported in the literature [11–19]. There is also a patient with EP who was presented with sudden sensorineural hearing loss and tinnitus, although EP was not

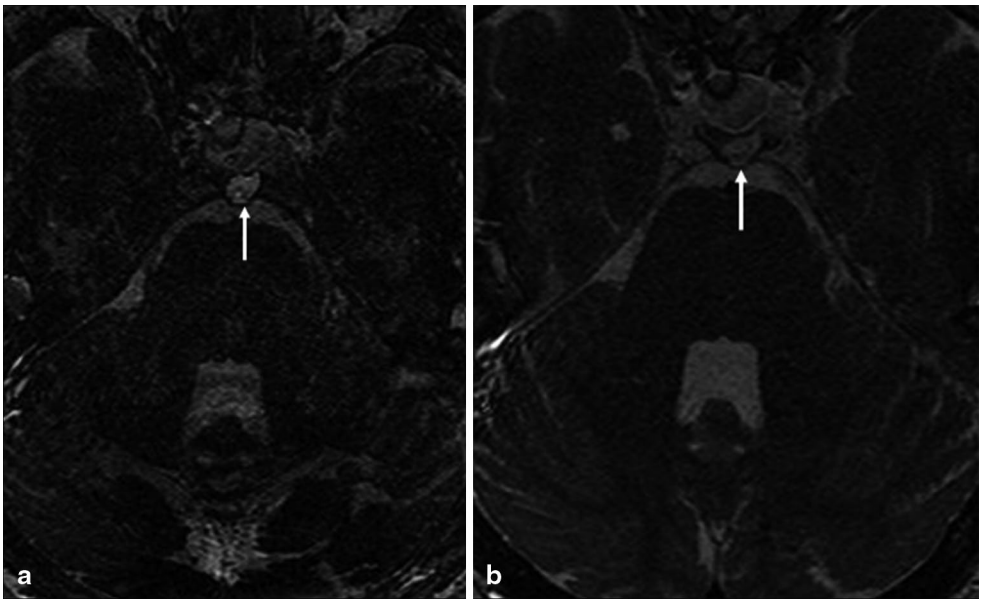

Fig. 4 Ecchordosis physaliphora variant in a 28-year-old man with hearing loss. Axial precontrast (**a**) and contrast-enhanced (**b**) fast imaging employing steady-state acquisition images demonstrate a nonenhancing hyperintense lesion within the clivus alone (*arrow*) at an upper level than the Dorello canal in the midline

found responsible for his otological symptoms [20]. EPs usually have a larger size in symptomatic patients in contrast to the relatively smaller size of the incidentally discovered lesions. The largest (15 × 8 × 18 mm) EP in our study was occupying the prepontine cistern of a patient with tinnitus (Fig. 2). However, given the absence of the prominent mass effect on the brainstem or direct contact to the vestibulocochlear nerve, the symptom of the patient was less likely associated with EP. We found no direct relationship between the EP and the symptoms in other patients as well. Although it seems that otological symptoms are questionably associated with EP, slightly higher incidence of the lesion on temporal MR images is notable.

Most classical type A EPs in our study were oval-shaped, well-defined lesions in the retroclival region consistent with the literature data. In three of these lesions, adjacent arteries were causing focal displacement on the wall of the EPs. This finding may reflect the cystic nature of the lesion and be useful in distinguishing EP from chordoma, especially in patients without contrast-enhanced images. Except oval-shaped lesions, we also detected two lobulated EP located in axial and sagittal planes, respectively.

Classical type B EP is defined as a hyperintense lesion within the clivus associated with the type A lesion. Chihara et al. [4] reported 4 (23.5 %) type B lesion out of 17 classical EPs, where we found 4 (36.4 %) type B lesions in 11 classical EPs. Of these 4 lesions, two hyperintense lesions within the clivus had a bifid appearance caused by a midline bony segment, a finding not reported previously.

EP is attached to the posterior surface of the clivus with a tiny osseous stalk best seen on computed tomography (CT) [21]. T2-hypointense protrusion of the clivus is thought as the corresponding MR appearance of this osseous stalk. In our study, this finding was available in 9 (81.8 %) of the 11 classical EP. Chihara et al. [4] also found similar incidence (82.4 %) in their study. In addition, we determined T2-hypointense protrusion of the clivus without cyst-like component (incomplete EP) in 19 patients. Although this study was not designed to compare the utility of precontrast FIESTA and contrast-enhanced FIESTA images, it is notable that incomplete EPs were more recognizable on contrast-enhanced FIESTA images at least in patients with prominent basilar venous plexus. The basilar venous plexus is the venous channel with variable size overlying the dorsal clivus [22]. The cortex of the clivus and the basilar venous plexus have similar low signal intensities on precontrast FIESTA; however, T2-hypointense protrusion of the clivus is distinguished from the adjacent enhancing venous plexus confidently on FIESTA images following gadolinium administration.

We found hyperintense lesion within the clivus alone in only one case. The lesion was located in the midline at an upper level than the Dorello canal. Chihara et al. [4] found six lesions within the clivus alone. As most of these lesions were located at the Dorello canal level, they classified these lesions as EP variant. However, four (66.6 %) of the six EP variant lesions were located off-midline, while all classical and incomplete EPs (a total of 72 lesions) were at the midline in their study. We consider that being in an off-midline location with such a high percentage (66.6 %) is a suspicious finding for a notochord-related lesion such as EP. The notochord reaches the posterior clivus, the pharyngeal surface, and the dorsum sella in its anatomical path in the skull base during embryological development [23, 24]. Thornwaldt's cyst, anatomic variations such as fossa navicularis and canalis basilaris medianus, and neoplasms such as chordoma and benign notochordal cell tumor are all notochord-related lesions with a characteristic midline location [24–27]. How-

ever, in rare instances, chordomas may arise off the midline in the petrous apex [28]. This finding is most likely related to the remnants of the notochordal branches that penetrate the skull base in different directions during the multiplication of the notochordal cells in the early embryogenic stage [28]. Although this theory explains the off-midline location of a notochord-related lesion, we are still in doubt to define an off-midline-located intraclival lesion as EP confidently considering the relatively high percentage of these lesions in the previous study. In addition, it is also difficult to distinguish EP variant from benign notochordal cell tumor based on MR findings because both lesions show hyperintensity on T2-weighted images and no contrast enhancement [26, 27]. In such cases, CT may be helpful because benign notochordal cell tumors usually manifest as mild osteosclerosis on CT [26, 27]. Unfortunately, CT was not available in our patient with EP variant. As a result, in our opinion, a diagnosis of EP variant as proposed by Chihara et al. [4] is contraversial due to the uncertainty of the notochordal origin of a off-midline-located lesion and the possibility of a benign notochordal cell tumor even in the presence of a midline lesion.

The major clinically significant point in cases with EP is to distinguish the lesion from chordoma. Both are notochord-related lesions with similar MR signal characteristics (hypointense on T1-weighted images and hyperintense on T2-weighted images); however, chordoma is a malignant tumor with aggressive behavior in contrast to the benign nature of EP [29]. Therefore, chordomas are usually symptomatic lesions showing contrast enhancement and extensive bone destruction, whereas EPs are nonenhancing incidental lesions [29]. Although chordomas mostly occur in extradural location, rarely, they may be seen as an intradural retroclival lesion and confused with EP. Intradural chordomas usually do not present bony involvement [30]. In addition, both intradural chordoma and EP have similar histological features, and there is no reliable follow-up criteria indicating the stability of these entities [30]. In such cases, the presence of contrast enhancement, a suggestive feature of chordoma, may be the only hint in distinguishing intradural chordoma from EP. In our study, we believe that diagnosis of chordoma was confidently excluded because all lesions were evaluated by contrast-enhanced images and none showed enhancement in our study population. One small midline lesion with retroclival and intraclival components was not included in the study due to the contrast enhancement on contrast-enhanced FIESTA and T1-weighted images. This lesion was hypointense on T1-weighted image and hyperintense on T2-weighted image; however, unlike hyperintense cyst-like appearance of a classical EP, its signal intensity was low on precontrast FIESTA image. We evaluated the lesion as a possible chordoma based on imaging findings; however, no histopathological confirmation was available in the medical records of our hospital. Surprisingly, we found no data regarding the imaging features of intradural chordoma on CISS/FIESTA imaging in radiology literature. Therefore, in our opinion, further investigations focusing on the signal intensity of chordoma on CISS/FIESTA imaging may provide additional information on the discrimination of these notochord-related lesions.

There are several limitations in this study. First, our study was retrospective. Second, both the sample size and the total number of EPs were small when compared with the study of Chihara et al. [4]. In contrast, we detected more lesions in a larger study population than those found by Mehnert et al. [3]. Third, imaging pathological correlation was not available because EP was not considered as the cause of the otological symptoms. Moreover, inconsistencies in radiological evaluation were resolved by consensus, and a bias between observers could not be entirely excluded. In addition, CT data were available in only three patients; therefore, T2-hypointense protrusions of the clivus could not be confirmed as osseous stalk on CT in most of the patients.

In conclusion, we found many EPs in patients with otological symptoms on temporal MR imaging using precontrast and contrast-enhanced FIESTA images. We described various imaging appearances in EP consistent with the results of the study by Chihara et al. [4]; however, the incidence of classical EP was slightly higher than those found by the previous studies. Contrast-enhanced FIESTA images were helpful not only to rule out chordoma but also in clear visualization of T2-hypointense protrusions of the clivus. Therefore, with the added value of contrast-enhanced images, classification proposed by Chihara et al. [4] may be an advisable method in the assessment of EP, although we find EP variant lesions questionable.

Sources of Funding None.

Conflict of Interest The authors declare that there are no actual or potential conflicts of interest in relation to this article.

References

1. Wolfe JT, III, Scheithauer BW. “Intradural chordoma” or “giant ecchordosis physaliphora”? Report of two cases. Clin Neuropathol. 1987;6:98–103.
2. Rodriguez L, Colina J, Lopez J, Molina O, Cardozo J. Intradural prepontine growth: giant ecchordosis physaliphora or extraosseous chordoma? Neuropathology. 1999;19:336–40.
3. Mehnert F, Beschorner R, Kuker W, Hahn U, Nagele T. Retroclival ecchordosis physaliphora: MR imaging and review of the literature. AJNR Am J Neuroradiol. 2004;25:1851–55.
4. Chihara C, Korogi Y, Kakeda S, Nishimura J, Murakami Y, Moriya J, Ohnari N. Ecchordosis physaliphora and its variants: proposed new classification based on high-resolution fast MR imaging employing steady-state acquisition. Eur Radiol. 2013;23:2854–60.

5. Chavhan GB, Babyn PS, Jankharia BG, Cheng HL, Shroff MM. Steady-state MR imaging sequences: physics, classification, and clinical applications. Radiographics. 2008;28:1147–60.
6. Sheth S, Branstetter BF, 4th, Escott EJ. Appearance of normal cranial nerves on steady-state free precession MR images. Radiographics. 2009;29:1045–55.
7. Shigematsu Y, Korogi Y, Hiari T, Okuda T, Ikushima I, Sugahara T, Liang L, Takahashi M. Contrast-enhanced CISS MRI of vestibular schwannomas: phantom and clinical studies. J Comput Asist Tomogr. 1999;23:224–31.
8. Yamamoto J, Kakeda S, Takashi M, Takahashi M, Aoyama Y, Soejima Y, Saito T, Akiba D, Korogi Y, Nishizawa S. Dural attachment of intracranial meningiomas: evaluation with contrast-enhanced three-dimensional fast imaging with steady-state acquisition (FIESTA) at 3T. Neuroradiology. 2011;53:413–23.
9. Amemiya S, Aoki S, Ohtoma K. Cranial nerve assessment in cavernous sinus tumors with contrast-enhanced 3D fast-imaging employing steady-state acquisition MR imaging. Neuroradiology. 2009;51:467–70.
10. Hayashi M, Ochiai T, Nakaya K, Chernov M, Tamura N, Yomo S, Izawa M, Hori T, Takakura K, Regis J. Image-guided microradiosurgery for skull base tumors: advantages of using gadolinium-enhanced constructive interference in steady-state imaging. J Neurosurg. 2006;105:12–7.
11. Cha ST, Jarrahy R, Yong WH, Eby T, Shahinian HK. A rare symptomatic presentation of ecchordosis physaliphora and unique endoscope-assisted surgical management. Minim Invasive Neurosurg. 2002;45:36–40.
12. Akimoto J, Takeda H, Hashimoto T, Haraoka J, Ito H. A surgical case of ecchordosis physaliphora [in Japanese]. No Shinkei Geka. 1996;24:1021–25.
13. Alkan O, Yildirim T, Kizilkiliç O, Tan M, Çekinmez M. A case of ecchordosis physaliphora presenting with an intratumoral hemorrhage. Turk Neurosurg. 2009;19:293–6.
14. Macdonald RL, Cusimano MD, Deck JH, Gullane PJ, Dolan EJ. Cerebrospinal fluid fistula secondary to ecchordosis physaliphora. Neurosurgery. 1990;26:515–9.
15. Dias L, Nakanishi M, Mangussi-Gomes J, Canuto M, Takano G, Oliveira CA. Successful endoscopic endonasal management of a transclival cerebrospinal fluid fistula secondary to ecchordosis physaliphora—an ectopic remnant of primitive notochord tissue in the clivus. Clin Neurol Neurosurg. 2014;117:116–9.
16. Stam FC, Kamphorst W. Ecchordosis physaliphora as a cause of fatal pontine hemorrhage. Eur Neurol. 1982;21:90–3.
17. Fracasso T, Brinkman B, Paulus W. Sudden death due to subarachnoid bleeding from ecchordosis physaliphora. Int J Legal Med. 2008;122:225–7.
18. Krisht KM, Palmer CA, Osborn AG, Couldwell WT. Giant ecchordosis physaliphora in an adolescent girl: case report. J Neurosurg Pediatr. 2013;12:328–33.
19. Yamamoto T, Yano S, Hide T, Kuratsu J. A case ecchordosis of physaliphora presenting with an abducens nerve palsy: a rare symptomatic case managed with endoscopic endonasal transsphenoidal surgery. Surg Neurol Int. 2013;4:13.
20. Ling SS, Sader C, Robbins P, Rajan GP. A case of giant ecchordosis physaliphora: a case report and literature review. Otol Neurotol. 2007;28:931–3.
21. Bag AK, Chapman PR. Neuroimaging: intrinsic lesions of the central skull base region. Semin Ultrasound CT MR. 2013;34:412–35.
22. Tubbs RS, Hansasuta A, Loukas M, et al. The basilar venous plexus. Clin Anat. 2007;20:755–9.
23. Laine FJ, Nadel L, Braun IF. CT and MR imaging of the central skull base. Part 1: techniques, embryological development, and anatomy. Radiographics. 1990;10:591–602.
24. Lohman BD, Sarikaya B, Mckinney AM, Hadi M. Not the typical Thornwaldt's cyst this time. A nasopharyngeal cyst associated with canalis basilaris medianus. Br J Radiol. 2011;84:169–171.
25. Cankal F, Ugur FC, Tekdemir I, Elhan A, Karahan T, Sevim A. Fossa navicularis: anatomic variation at the skull base. Clin Anat. 2004;17:118–22.
26. Nishiguchi T, Mochizuki K, Ohsawa M, Inoue T, Kageyama K, Suzuki A, Takami T, Miki Y. Differentiating benign notochordal cell tumors from chordomas: radiographic features on MRI, CT, and tomography. AJR Am J Roentgenol. 2011;196:644–50.
27. Iorgulescu JB, Laufer I, Hameed M, Boland P, Yamada Y, Lis E, Bilsky M. Benign notochordal cell tumors of the spine: natural history of 8 patients with histologically confirmed lesions. Neurosurgery. 2013;73:411–6.
28. Brown RW, Sage MR, Brophy BP. CT and MR findings in patients with chordomas of the petrous apex. AJNR Am J Neuroradiol. 1990;11:121–4.
29. Erdem E, Angtuaco EC, Van Hemert R, Park JS, Al-Mefty O. Comprehensive review of intracranial chordoma. Radiographics. 2003;23:995–1009.
30. Bhat DI, Yasha M, Rojin A, Sampath S, Shankar SK. Intradural clival chordoma: a rare entity. J Neurooncol. 2010;96:287–90.